NASA TM X-44

TECHNICAL MEMORANDUM

X - 44

EFFECTS OF WING VERTICAL LOCATION ON THE STABILITY AND CONTROL CHARACTERISTICS AT A MACH NUMBER OF 2.01 OF A CANARD AIRPLANE CONFIGURATION WITH A TRAPEZOIDAL ASPECT-RATIO-3 WING

By Gerald V. Foster

Langley Research Center
Langley Field, Va.

CLASSIFIED DOCUMENT - TITLE UNCLASSIFIED

This material contains information affecting the national defense of the United States within the meaning of the espionage laws, Title 18, U.S.C., Secs. 793 and 794, the transmission or revelation of which in any manner to an unauthorized person is prohibited by law.

NATIONAL AERONAUTICS AND SPACE ADMINISTRATION
WASHINGTON

September 1959

NATIONAL AERONAUTICS AND SPACE ADMINISTRATION

TECHNICAL MEMORANDUM X-44

EFFECTS OF WING VERTICAL LOCATION ON THE STABILITY AND CONTROL CHARACTERISTICS AT A MACH NUMBER OF 2.01 OF A CANARD AIRPLANE CONFIGURATION WITH A TRAPEZOIDAL ASPECT-RATIO-3 WING*

By Gerald V. Foster

SUMMARY

An investigation has been conducted in the Langley 4- by 4-foot supersonic pressure tunnel to determine the effects of wing vertical location on the longitudinal and directional stability characteristics of a canard airplane configuration at a Mach number of 2.01. The wing had a trapezoidal plan form of aspect ratio 3, a taper ratio of 0.25, and 4-percent-thick circular-arc airfoil sections. The configurations investigated included a high-wing and a low-wing arrangement.

Change in wing vertical location had no significant effect on the longitudinal aerodynamic characteristics of the canard-surface-off configurations; however, with the canard-surface-on configurations, decrease in wing vertical location resulted in a small increase in lift-curve slope with an accompanying increase in drag. For a static margin of zero both wing-location configurations had a maximum trimmed lift-drag ratio of 6.0 which gradually decreased with increased static margin. For values of static margin greater than approximately 0.20 mean geometric chord, a decrease in wing vertical location had an adverse effect on the maximum lift-drag ratio. The low-wing configuration with canard surfaces and vertical tail on possessed greater directional stability and less positive effective dihedral at low angles of attack than did the high-wing configuration. Both wing-location configurations were directionally unstable at high angles of attack. Canard-surface deflection resulted in a decrease in the directional stability of the low-wing configuration at low and moderate angles of attack and in a general increase in positive effective dihedral of both wing-location configurations.

*Title, Unclassified.

INTRODUCTION

An investigation is currently being conducted in the Langley 4- by 4-foot supersonic pressure tunnel to determine the aerodynamic characteristics of several canard airplane configurations at supersonic speeds. Consideration of the effects of wing plan form, canard-surface size, wing trailing-edge flap control, and forebody length on the longitudinal, directional, and lateral stability characteristics of a canard airplane configuration at supersonic Mach numbers is given in references 1, 2, 3, and 4, respectively. The effects of various components of configurations utilized in reference 1 are discussed in reference 5. The investigation has subsequently been extended to ascertain the effect of the vertical location of the wing on the aerodynamic characteristics of a canard airplane configuration at a Mach number of 2.01. The configuration used in this phase of the investigation was identical to the intermediate forebody-length version employed in reference 4.

The results presented herein include longitudinal and lateral aerodynamic characteristics of a high-wing and a low-wing configuration with and without canard surfaces and vertical tail. In addition, the results include longitudinal control characteristics of both wing-body configurations. Some of these results have previously been reported in reference 6 as a part of a summary pertaining to the effects of various factors on the stability and performance characteristics of canard airplane configurations.

SYMBOLS

The longitudinal stability characteristics are referred to the stability-axis system (fig. 1(a)), whereas the lateral stability characteristics are referred to the body-axis system (fig. 1(b)). The reference center of moments was located 67.5 percent of the body length rearward of the nose (fig. 2). The symbols are defined as follows:

C_L lift coefficient, F_L/qS

C_D' drag coefficient, F_D'/qS

C_m pitching-moment coefficient, $M_{Y_s}/qS\bar{c}$

C_l rolling-moment coefficient, M_X/qSb

C_n yawing-moment coefficient, M_Z/qSb

C_Y	side-force coefficient, F_Y/qS
F_L	lift force
F_D'	drag force
F_Y	side force
M_{Y_s}	moment about Y-axis
M_X	moment about X-axis
M_Z	moment about Z-axis
S	wing area
b	wing span
$\bar{c}$	wing mean geometric chord
q	free-stream dynamic pressure
α	angle of attack, deg
β	angle of sideslip, deg
δ_c	canard-surface deflection with respect to body center line, positive when trailing edge down, deg
C_{n_β}	directional stability derivative per degree, $\partial C_n/\partial\beta$
C_{l_β}	rolling-moment derivative per degree, $\partial C_l/\partial\beta$
C_{Y_β}	side-force derivative per degree, $\partial C_Y/\partial\beta$
L/D	lift-drag ratio

Subscript:

max	maximum

Components:

W	wing
B	body
C	canard surface
V	vertical tail

MODEL AND APPARATUS

Details of the model are shown in figures 2 and 3. The geometric characteristics are presented in table I. The body of the model was composed of a parabolic nose followed by a frustum of a cone which was faired into a cylinder. The fineness ratio of the body was 11.1. The coordinates of the body are presented in reference 4. The canard surfaces were trapezoidal in plan form with an exposed area equal to 7.07 percent of the wing area. The canard surfaces were deflected by remote control about a hinge line located at a station 24.6 percent of the body length rearward of the nose. The airfoil sections of the canard surfaces were hexagonal, whereas the wing was composed of circular-arc sections. The wing was attached to the body in either a high or low location. (See fig. 2.) The body-mounted vertical tail had 60° sweepback at the leading edge, an aspect ratio of 1.11, and was located so that the trailing edge of the exposed root chord would be coincident with the body base. Force and moment measurements were made through the use of a six-component internal strain-gage balance attached to a rotary-type sting.

TESTS, CORRECTIONS, AND ACCURACY

The conditions for the tests were as follows:

Mach number	2.01
Stagnation pressure, lb/sq in. abs	10
Stagnation temperature, °F	100
Reynolds number, based on $\bar{c}$	1.85×10^6

The stagnation dewpoint was maintained sufficiently low (-25° F or less) so that no significant condensation effects would be encountered in the test section.

The sting angle was corrected for deflection of the sting and balance under load. The base pressure was measured and the chord force was adjusted to a base pressure equal to the free-stream static pressure.

The estimated maximum variations in the individual measured quantities are as follows:

C_L	±0.0003
C_D'	±0.0010
C_m	±0.0004
C_l	±0.0004
C_n	±0.0001
C_Y	±0.0015
α, deg	±0.2
β, deg	±0.2
δ_c, deg	±0.1

The Mach number variation in the test section was approximately ±0.01, and the flow-angle variation in the vertical and horizontal planes was within approximately ±0.1°.

PRESENTATION OF RESULTS

	Figure
Aerodynamic characteristics in pitch for various combinations of components. High wing	4
Aerodynamic characteristics in pitch for various combinations of components. Low wing	5
Effect of canard-surface deflection on aerodynamic characteristics in pitch. High wing	6
Effect of canard-surface deflection on aerodynamic characteristics in pitch. Low wing	7
Effect of wing vertical location on trim longitudinal characteristics. $\partial C_m/\partial C_L = -0.25$	8
Effect of wing vertical location on variation of maximum trimmed lift-drag ratio with longitudinal stability	9
Comparison of sideslip derivatives of high-wing and low-wing configurations with and without vertical tail. $\delta_c = 0°$	10
Aerodynamic characteristics in sideslip for various combinations of components. High wing	11
Aerodynamic characteristics in sideslip for various combinations of components. Low wing	12
Effect of canard-surface deflection on sideslip derivatives for complete model	13

DISCUSSION

Longitudinal Stability and Control Characteristics

A comparison of the results presented in figures 4 and 5 for the high- and the low-wing configurations indicates that variation in wing vertical location had no significant effect on the longitudinal aerodynamic characteristics of the canard-surface-off configuration; however, with the canard surface on, a decrease in wing location from the high to the low location resulted in a slight increase in lift-curve slope with an accompanying increase in drag. A comparison of the trim characteristics of the high-wing and the low-wing configurations based on a constant center-of-gravity location (fig. 8) indicates that a decrease in wing location resulted in a slight increase in the value of trimmed L/D at lift coefficient beyond that for maximum L/D. It would appear that the high-wing configuration was more adversely affected by the canard-surface wake than was the low-wing configuration. Both wing-location configurations had a maximum trimmed L/D of 5.55 for a constant static margin of $0.25\bar{c}$. Figure 9 indicates an increase in maximum trimmed L/D to about 6.0 for either complete wing-body configuration with a decrease in static margin to zero. This is approximately 0.6 less than the maximum lift-drag ratio of the canard-surface-off configurations. It may be noted that a decrease in wing location for values of static margin greater than approximately $0.20\bar{c}$ tends to have an adverse effect on the maximum trimmed L/D.

Lateral and Directional Stability Characteristics

Effect of wing vertical location.- The effects of wing vertical location on the sideslip derivatives of the models with and without a body-mounted vertical tail are shown in figure 10. Variations of C_n, C_l, and C_Y with β for the high-wing and low-wing configurations are presented in figures 11 and 12, respectively, for angles of attack of 0° and 13.2°. As would be expected, both wing-body configurations with the vertical tail off were directionally unstable; however, the instability of the high-wing configuration decreased with increase in angle of attack, whereas the directional stability derivative C_{n_β} of the low-wing configuration was approximately constant through the angle-of-attack range. The contribution of the vertical tail to C_{n_β} of both wing-body configurations decreased with increase in angle of attack; however, the magnitude of the contribution realized with the low-wing configuration at low angles of attack was substantially greater than that obtained with the high-wing configuration. As a result of this difference in tail contribution, C_{n_β} for the tail-on configuration

with the low wing was highest at low angles of attack. With increase in angle of attack, C_{n_β} of both wing-body configurations decreased and became zero at approximately 9°. It may be noted that although both wing-body configurations exhibited directional instability at high angles of attack, the degree of instability of the high-wing configuration was markedly less than that of the low-wing configuration because of the stabilizing tendency of the high-wing tail-off configuration.

The effects of wing vertical location on C_{n_β} of the canard airplane configuration were similar to those indicated for tail-rearward airplane configurations at subsonic and supersonic speeds. (For example, see refs. 7 to 11.) The effects of wing location have been associated with an induced sidewash arising from differential wing pressures in the region of the wing-body juncture. These flow disturbances have a stabilizing effect above the wing for the high-wing configuration and below the wing for the low-wing configuration.

The effects of wing vertical location on the effective dihedral C_{l_β} (fig. 10) of the canard airplane configuration are similar to effects obtained with tail-rearward airplane configurations at subsonic and supersonic speeds (refs. 7 to 11). With decrease in wing location from the high location to the low location, C_{l_β} of the wing-body configuration at $\alpha = 0°$ indicated that the effective dihedral changed from positive to negative. This change in effective dihedral is attributed to the effect of antisymmetric spanwise variation of angle of attack due to the body in sideslip (ref. 7). It may be noted that although the effective dihedral of both high-wing and low-wing configurations tended to become more positive with an increase in α, the effect of wing location on C_{l_β} is approximately constant through the range of α.

Effect of various components.- The results presented in figures 11 and 12 indicate that the addition of canard surfaces to either the high-wing or the low-wing configuration has no significant effect on the directional or lateral stability characteristics at $\alpha = 0°$. The results obtained at $\alpha = 13.2°$ indicate that the yawing moments of both the high-wing and low-wing configurations with canard surfaces and vertical tail on varied nonlinearly with sideslip angle. A comparison of the yawing-moment characteristics of the high-wing configuration with and without canard surfaces tends to indicate that the vertical tail is adversely affected by canard surfaces through a small range of sideslip angles near $\beta = 0°$ (fig. 11(b)). Similar effects of canard surfaces are shown in reference 5 for a wing-off configuration.

Effect of canard-surface deflection.- The effect of canard-surface deflection on the lateral and directional stability of the complete model

(fig. 13) indicates that a change in canard-surface deflection from 0° to 15° resulted in an increase in $-C_{l_\beta}$. This increase in $-C_{l_\beta}$ due to canard-surface deflection is approximately the same for both wing-body configurations. The canard-surface deflection also tends to have an adverse effect on the directional stability of the low-wing configuration at low and moderate angles of attack but to have no significant effect on C_{n_β} of the high-wing configuration. This decrease in C_{n_β} of the low wing is associated with canard-surface wake effects on the vertical tail, whereas the high wing appears to shield the vertical tail from the effects of the canard-surface wake.

CONCLUSIONS

An investigation of the effects of wing vertical location on the aerodynamic characteristics of a canard airplane configuration at a Mach number of 2.01 indicates the following conclusions:

1. Change in wing vertical location had no significant effect on the longitudinal aerodynamic characteristics of the canard-surface-off configuration; however, with the canard surfaces on, a decrease in wing location resulted in a small increase in lift-curve slope with an accompanying increase in drag.

2. A decrease in wing vertical location for a constant static margin (0.25 mean geometric chord) resulted in a small increase in trimmed lift-drag ratio at lift coefficients beyond that for maximum lift-drag ratio. By decreasing the static margin to zero, a maximum trimmed lift-drag ratio of 6.0 was obtained with either wing-location configuration. For a static margin greater than approximately 0.20 mean geometric chord, a decrease in wing location had an adverse effect on the maximum trimmed lift-drag ratio.

3. The low-wing configuration with canard surfaces and vertical tail on possessed greater directional stability and less positive effective dihedral at low angles of attack than did the high-wing configuration. Both wing-location configurations were directionally unstable at high angles of attack.

4. Canard-surface deflection resulted in a decrease in the directional stability of the low-wing configuration at low and moderate angles

of attack and in a general increase in positive effective dihedral of both wing-location configurations.

Langley Research Center,
National Aeronautics and Space Administration,
Langley Field, Va., April 20, 1959.

REFERENCES

1. Driver, Cornelius: Longitudinal and Lateral Stability and Control Characteristics of Two Canard Airplane Configurations at Mach Numbers of 1.41 and 2.01. NACA RM L56L19, 1957.

2. Spearman, M. Leroy, and Driver, Cornelius: Effects of Canard Surface Size on Stability and Control Characteristics of Two Canard Airplane Configurations at Mach Numbers of 1.41 and 2.01. NACA RM L57L17a, 1958.

3. Spearman, M. Leroy, and Driver, Cornelius: Longitudinal and Lateral Stability and Control Characteristics at Mach Number 2.01 of a 60° Delta-Wing Airplane Configuration Equipped With a Canard Control and With Wing Trailing-Edge Flap Controls. NACA RM L58A20, 1958.

4. Spearman, M. Leroy, and Driver, Cornelius: Effects of Forebody Length on the Stability and Control Characteristics at a Mach Number of 2.01 of a Canard Airplane Configuration With a Trapezoidal Aspect-Ratio-3 Wing. NASA MEMO 10-14-58L, 1958.

5. Driver, Cornelius: Longitudinal and Lateral Stability and Control Characteristics of Various Combinations of the Component Parts of Two Canard Airplane Configurations at Mach Numbers of 1.41 and 2.01. NASA MEMO 10-1-58L, 1958.

6. Spearman, M. Leroy, and Driver, Cornelius: Some Factors Affecting the Stability and Performance Characteristics of Canard Aircraft Configurations. NACA RM L58D16, 1958.

7. Goodman, Alex: Effects of Wing Position and Horizontal-Tail Position on the Static Stability Characteristics of Models With Unswept and 45° Sweptback Surfaces With Some Reference to Mutual Interference. NACA TN 2504, 1951.

8. Gillis, Clarence L., and Chapman, Rowe, Jr.: Effect of Wing Height and Dihedral on the Lateral Stability Characteristics at Low Lift of a 45° Swept-Wing Airplane Configuration As Obtained From Time-Vector Analyses of Rocket-Propelled-Model Flights at Mach Numbers From 0.7 to 1.3. NACA RM L56E17, 1956.

9. Heitmeyer, John C.: Effect of Vertical Position of the Wing on the Aerodynamic Characteristics of Three Wing-Body Combinations. NACA RM A52L15a, 1953.

10. Spearman, M. Leroy: Investigation of the Aerodynamic Characteristics in Pitch and Sideslip of a 45° Sweptback-Wing Airplane Model With Various Vertical Locations of the Wing and Horizontal Tail - Effect of Wing Location and Geometric Dihedral for the Wing-Body Combination, M = 2.01. NACA RM L55B18, 1955.

11. Robinson, Ross B.: Effects of Vertical Location of the Wing and Horizontal Tail on the Static Lateral and Directional Stability of a Trapezoidal-Wing Airplane Model at Mach Numbers of 1.41 and 2.01. NACA RM L58C18, 1958.

TABLE I.- GEOMETRIC CHARACTERISTICS OF MODEL

Body:	
Maximum diameter, in.	3.33
Length, in.	37.00
Base area, sq in.	8.71
Fineness ratio	11.1
Trapezoidal wing:	
Span, in.	24.00
Area, sq in.	192
Aspect ratio	3
Taper ratio	0.25
Mean geometric chord, in.	8.96
Sweep angle of leading edge	30° 58'
Sweep angle of 75-percent-chord line, deg	0
Airfoil section	Circular arc
Thickness-chord ratio	0.04
Canard:	
Total area, exposed, sq in.	13.59
Ratio of exposed area to wing area	0.0707
Airfoil section	Hexagonal
Constant thickness, in.	0.1875
Leading-edge angle, normal to leading edge, deg	10
Vertical tail:	
Total area, exposed, sq in.	23.42
Span, exposed, in.	5.10
Aspect ratio	1.11
Airfoil section	Wedge slab
Leading-edge angle, normal to leading edge, deg	10.6
Taper ratio	0.314

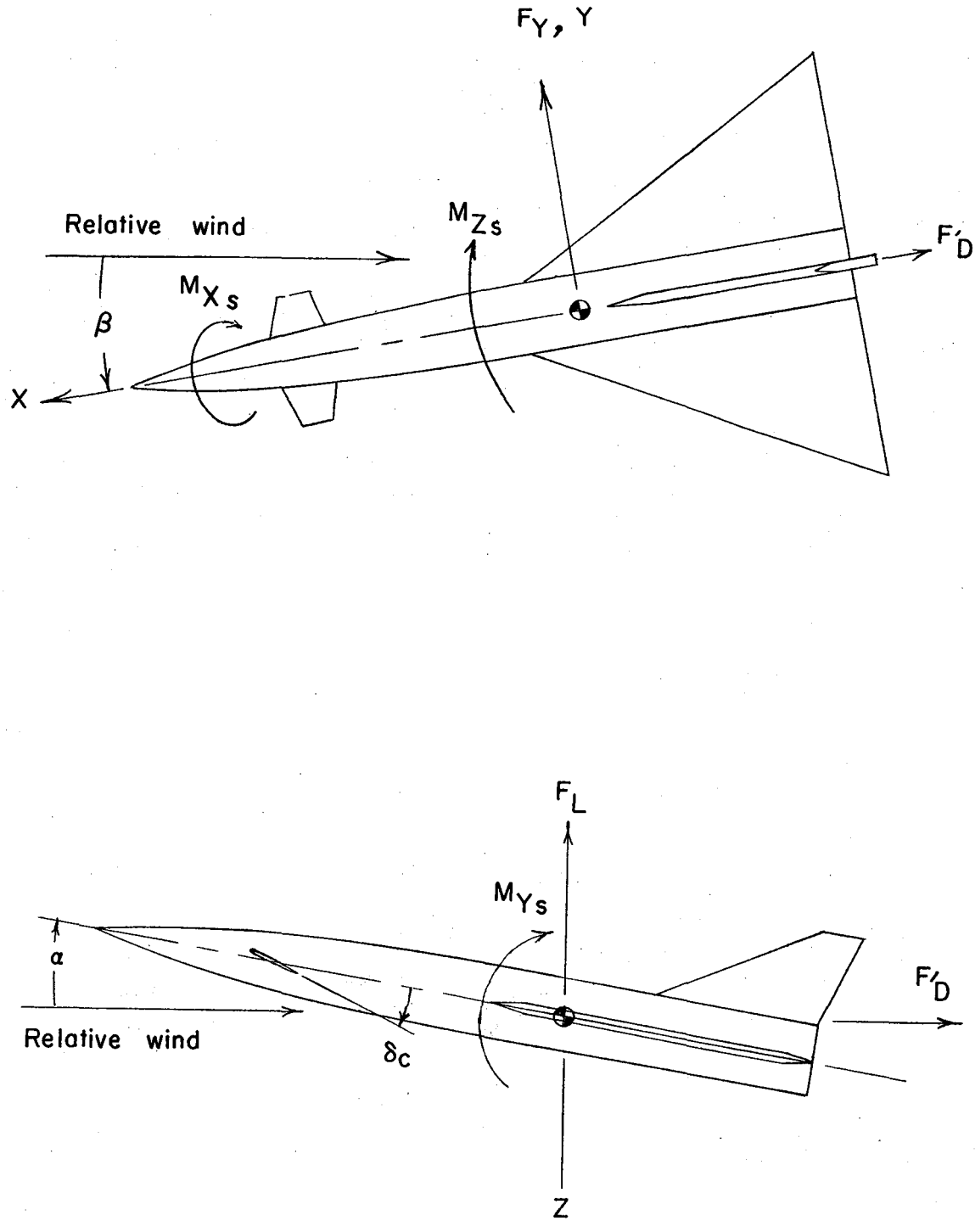

(a) Stability axes.

Figure 1.- Axis systems. Arrows indicate positive directions.

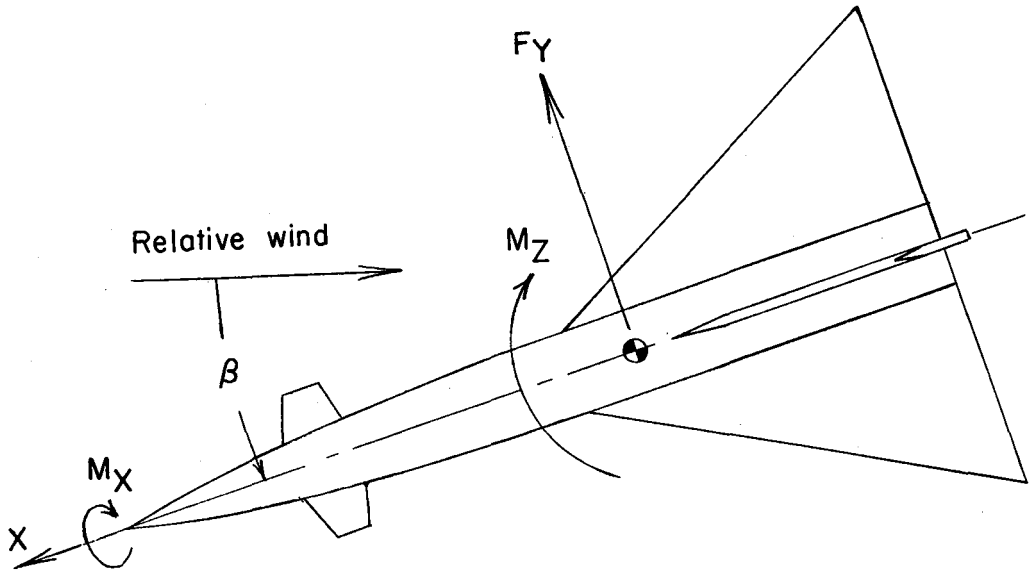

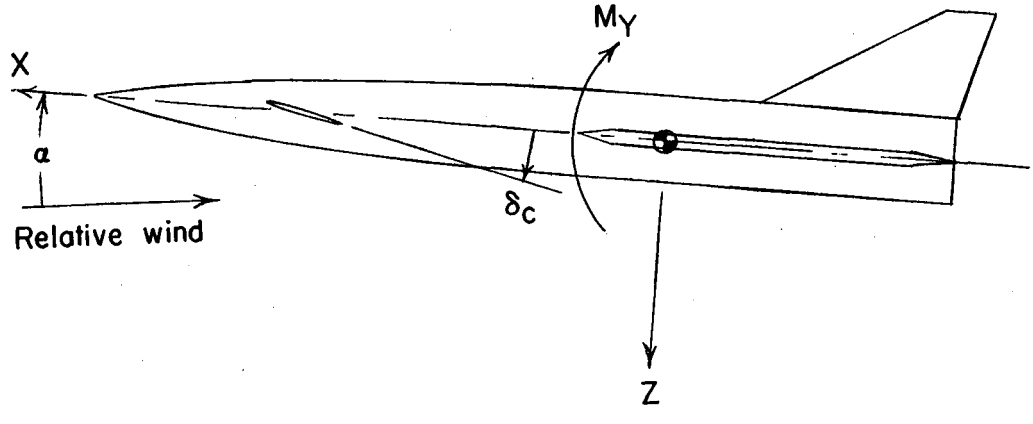

(b) Body axes.

Figure 1.- Concluded.

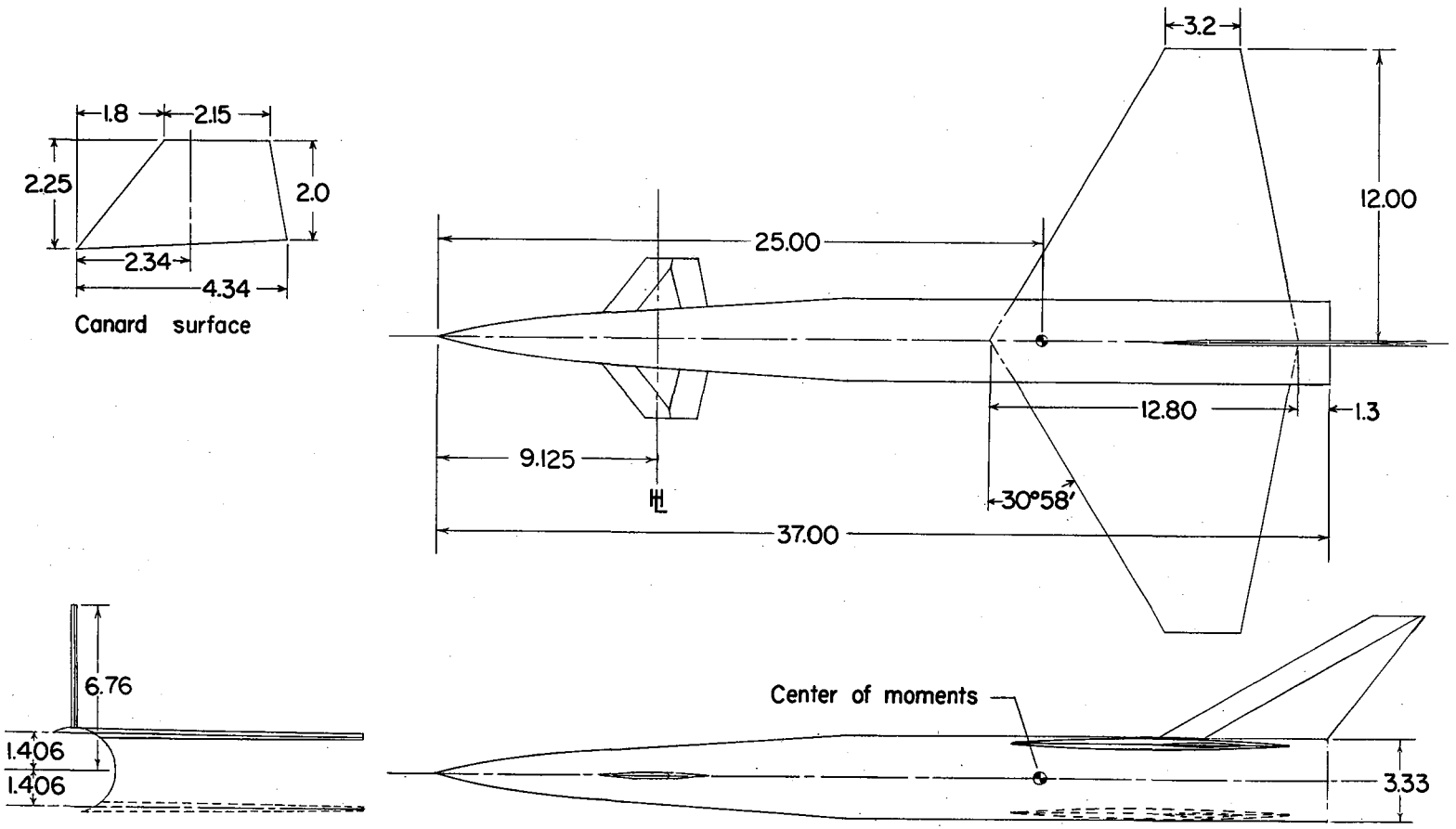

Figure 2.- Details of model. All dimensions are in inches unless otherwise specified.

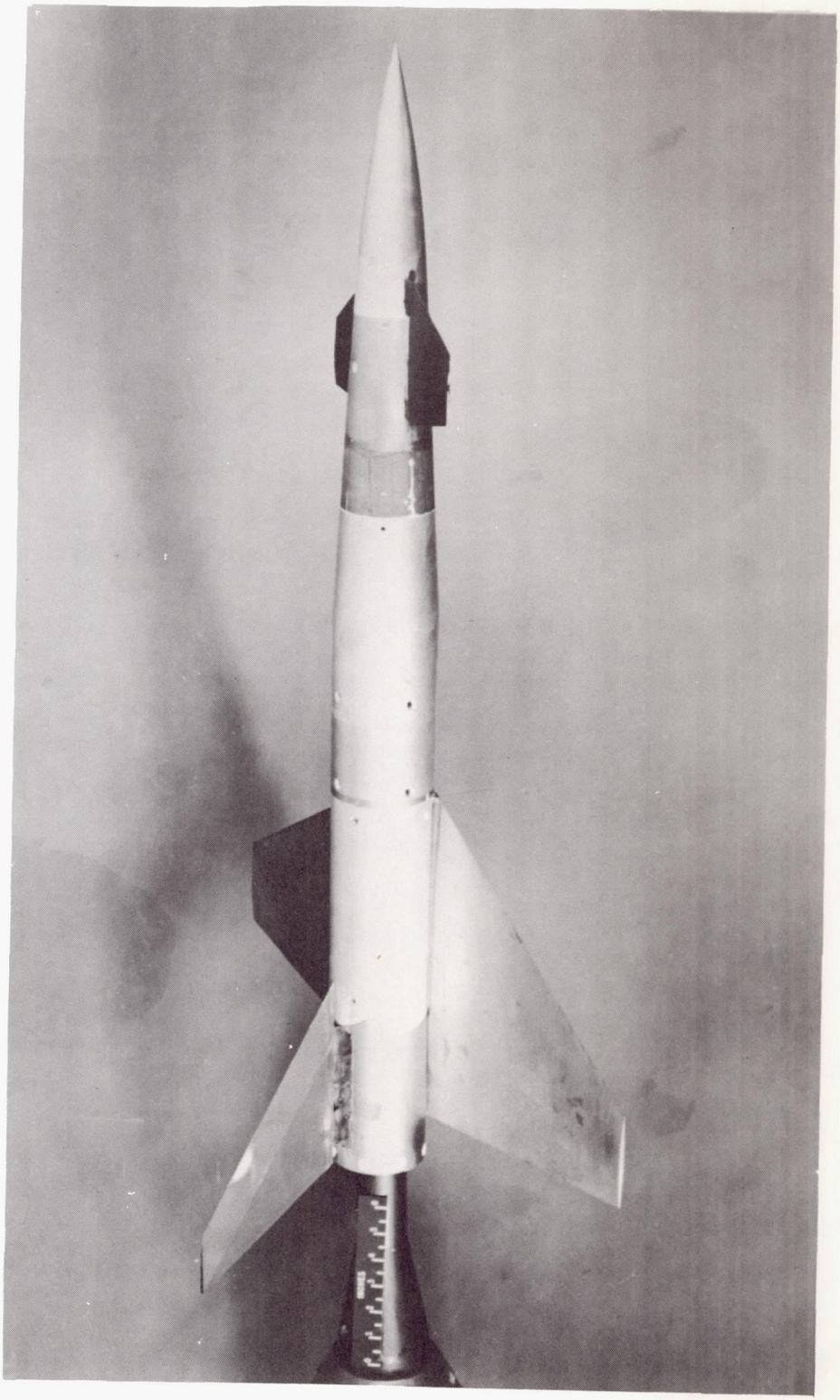

Figure 3.- Photograph of low-wing configuration. L-57-2679

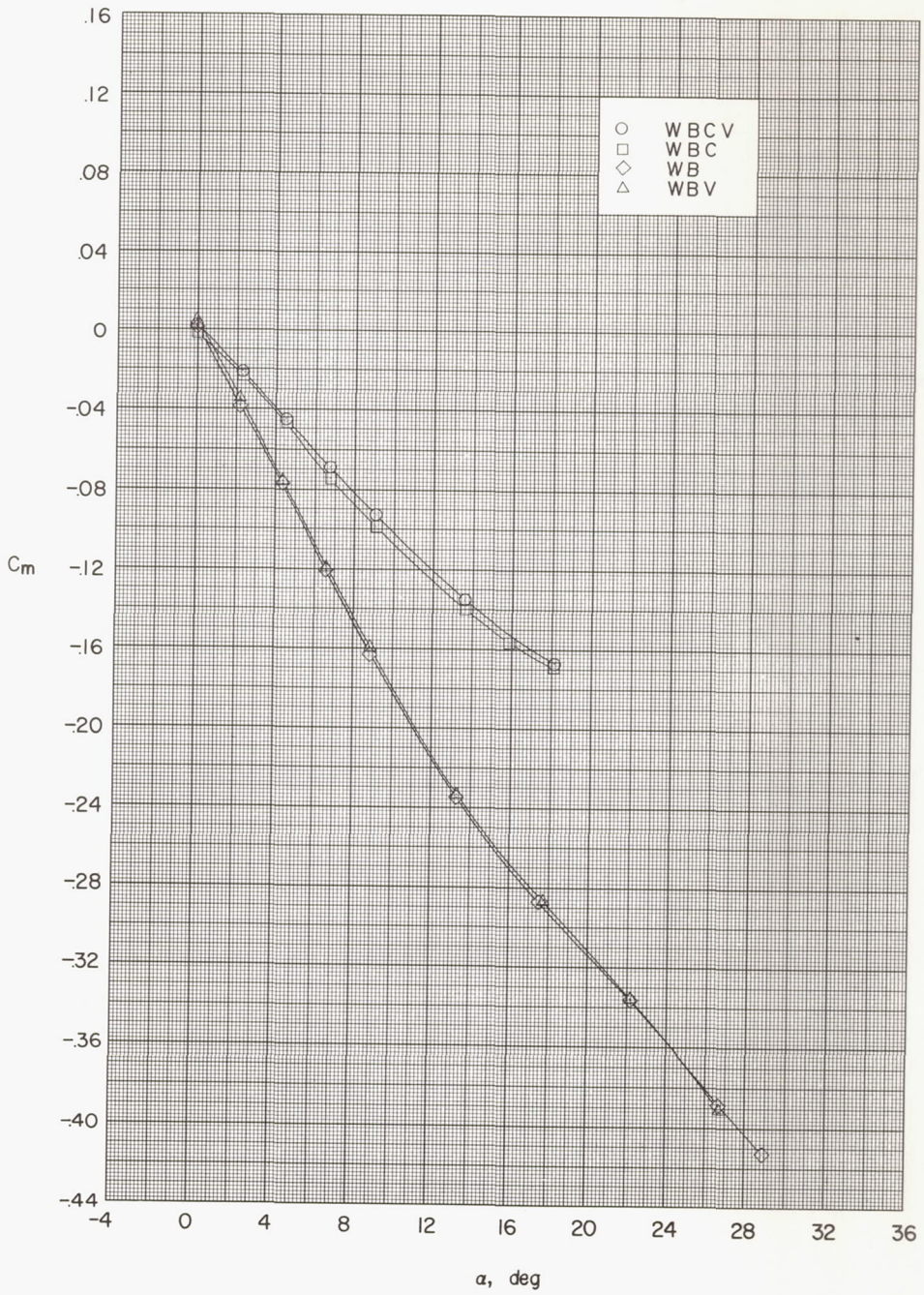

(a) Variation of C_m with α.

Figure 4.- Aerodynamic characteristics in pitch for various combinations of components. High wing.

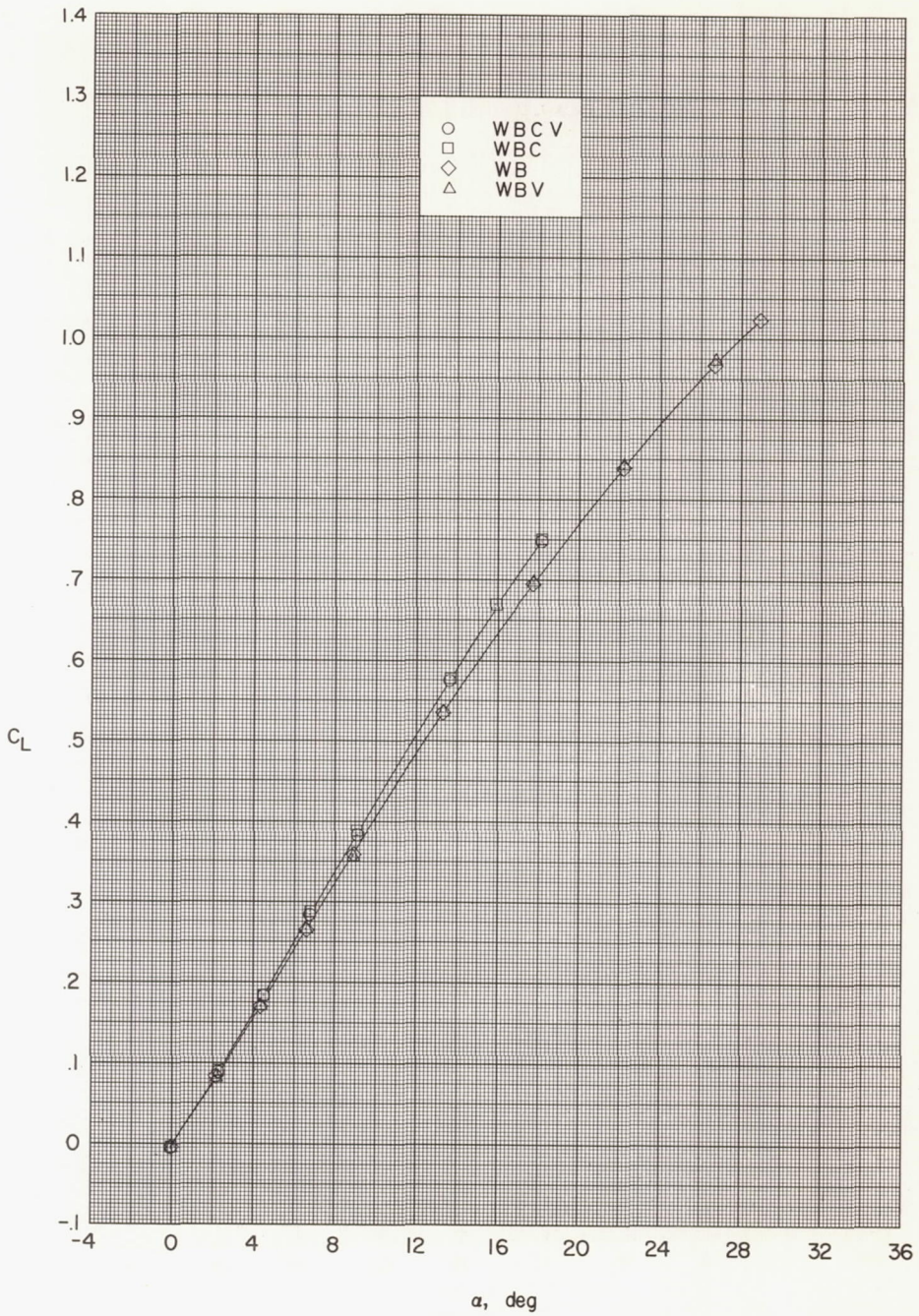

(b) Variation of C_L with α.

Figure 4.- Continued.

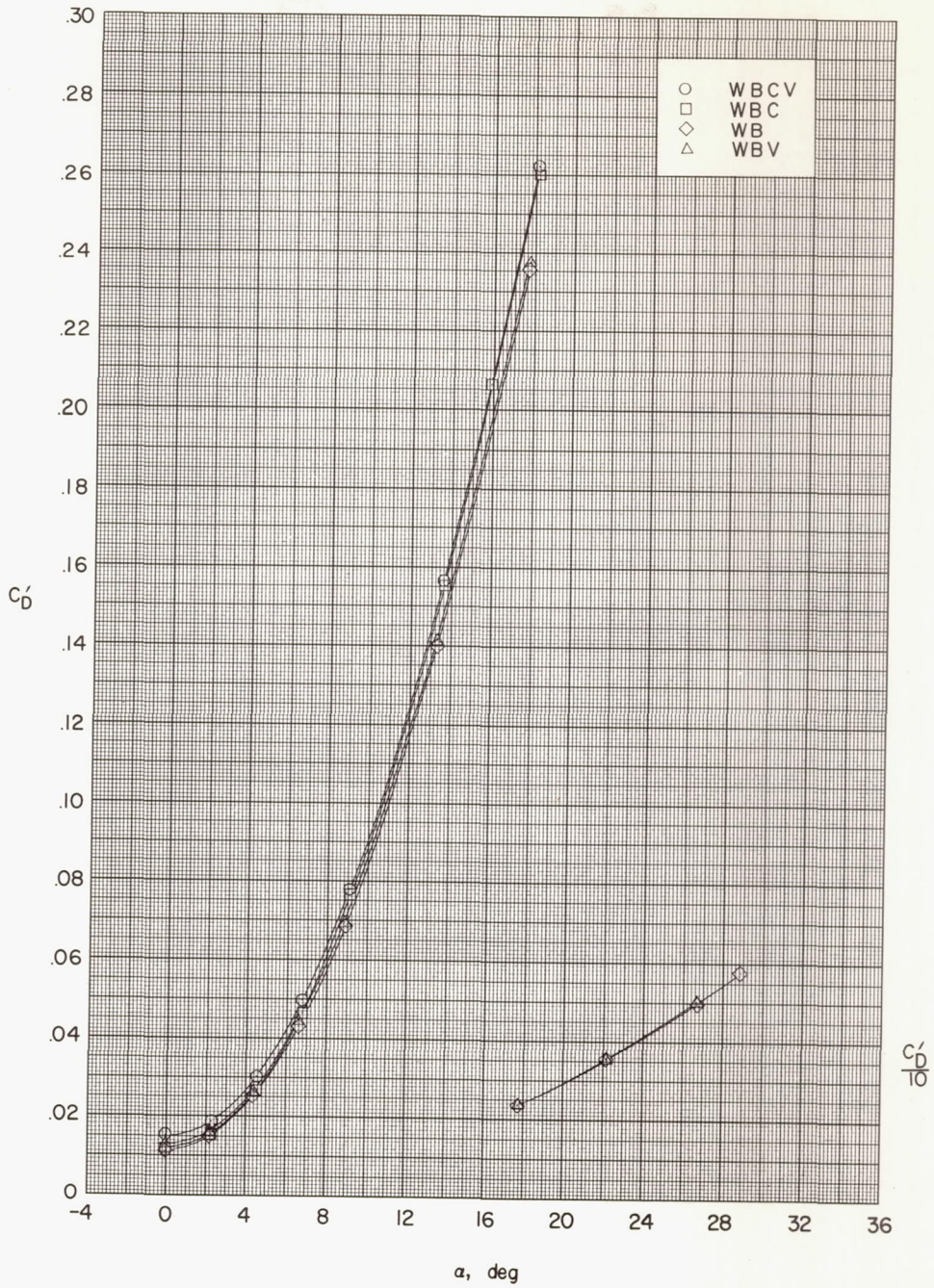

(c) Variation of C_D' with α.

Figure 4.- Concluded.

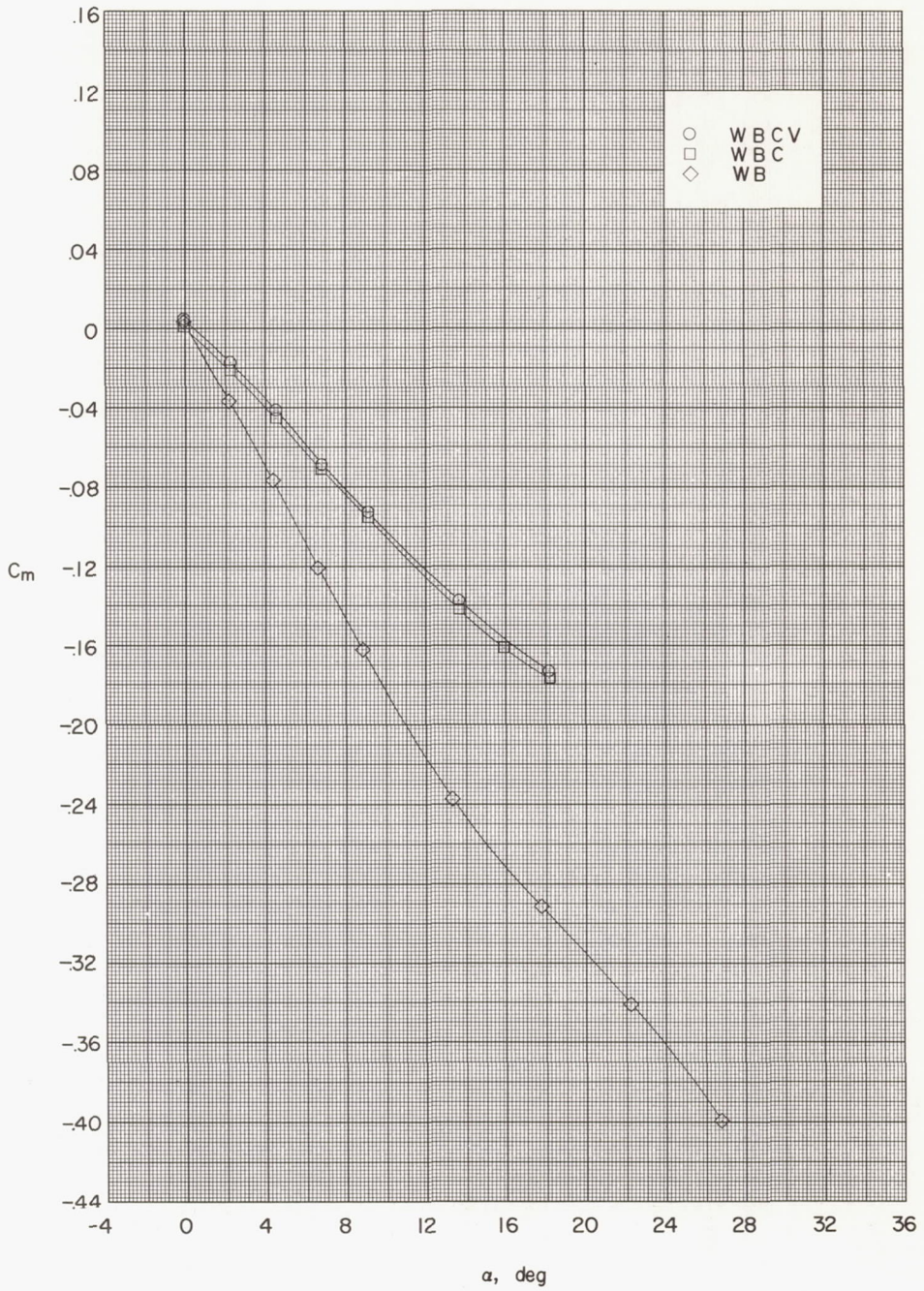

(a) Variation of C_m with α.

Figure 5.- Aerodynamic characteristics in pitch for various combinations of components. Low wing.

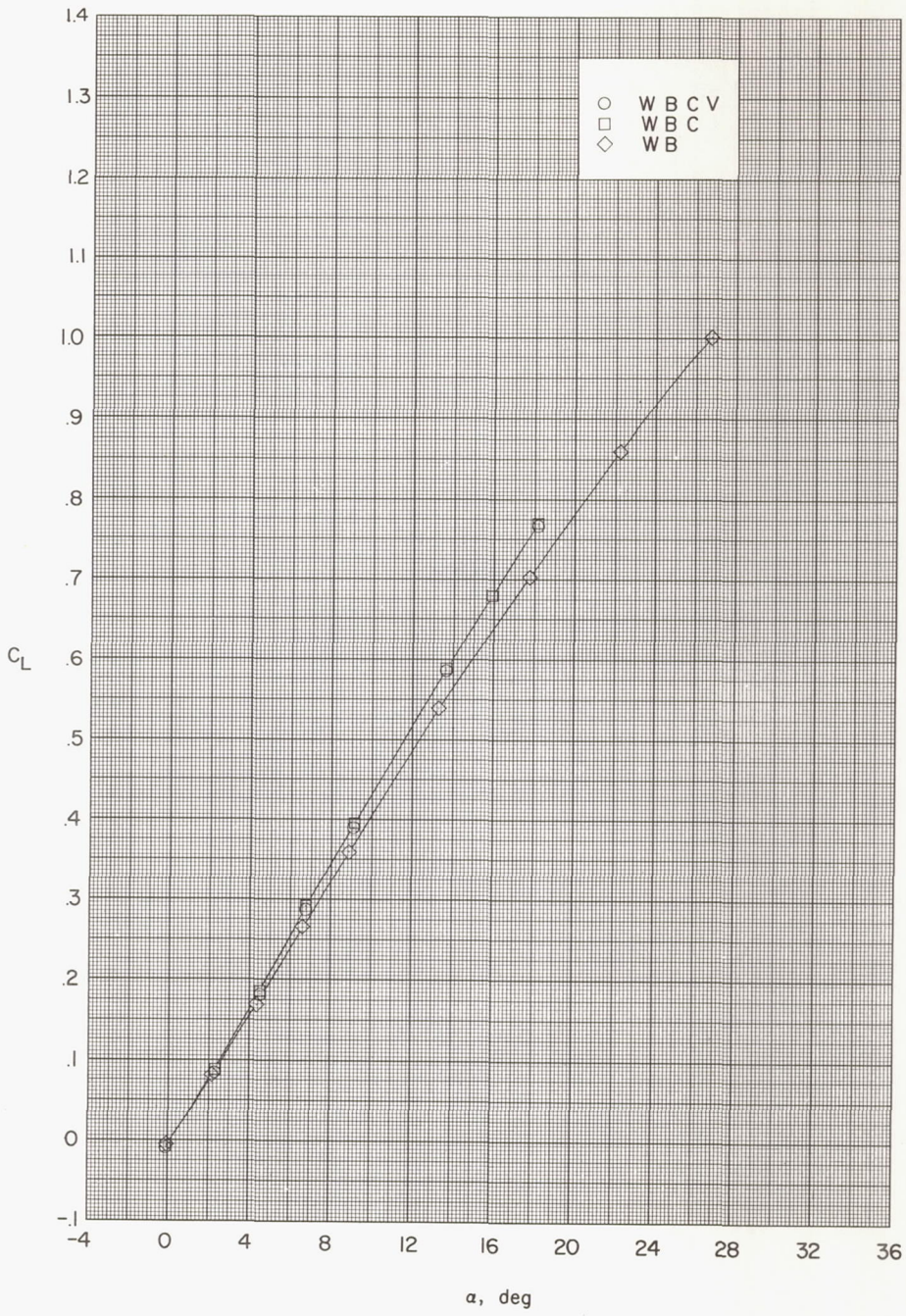

(b) Variation of C_L with α.

Figure 5.- Continued.

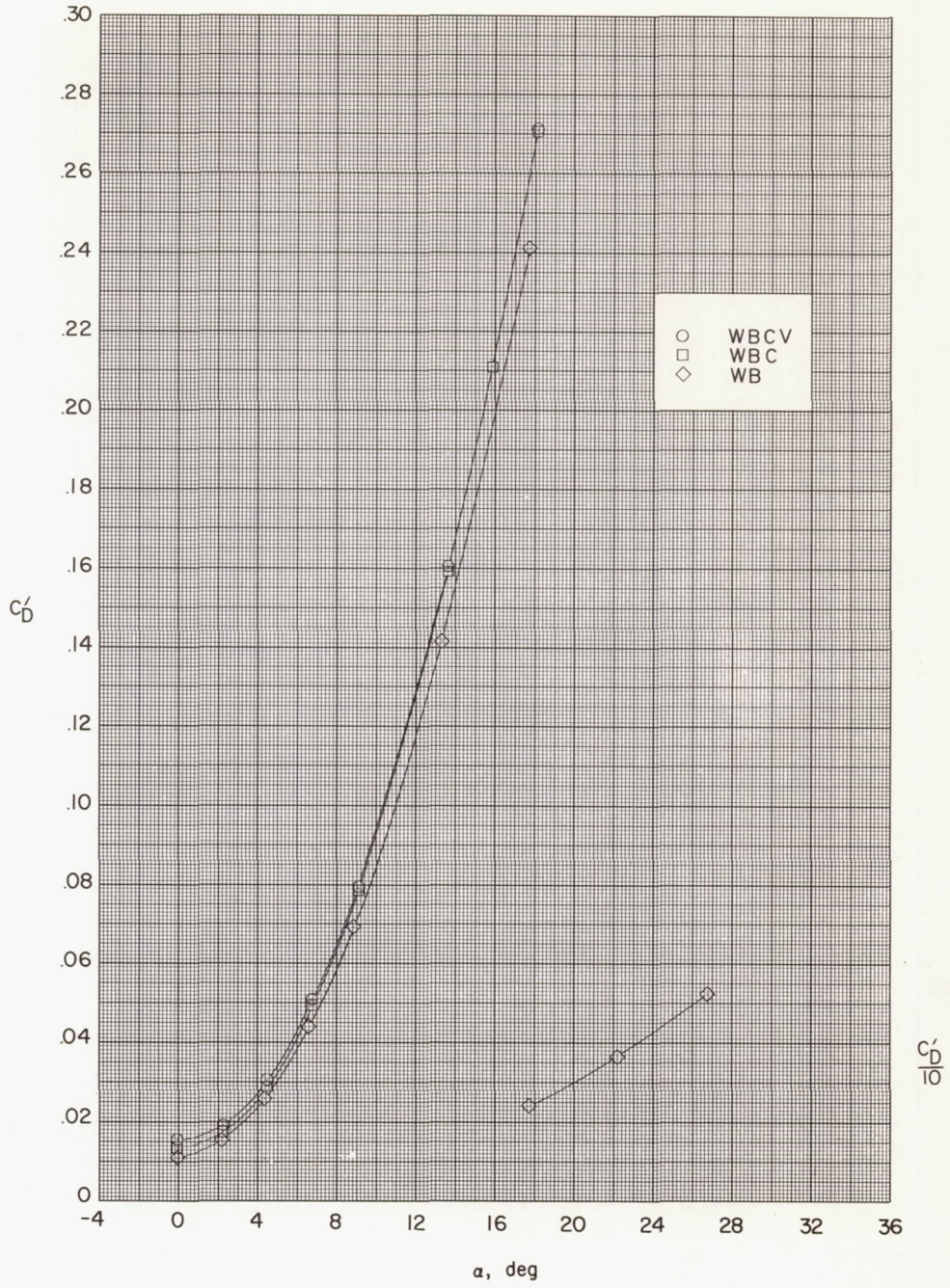

(c) Variation of C_D' with α.

Figure 5.- Concluded.

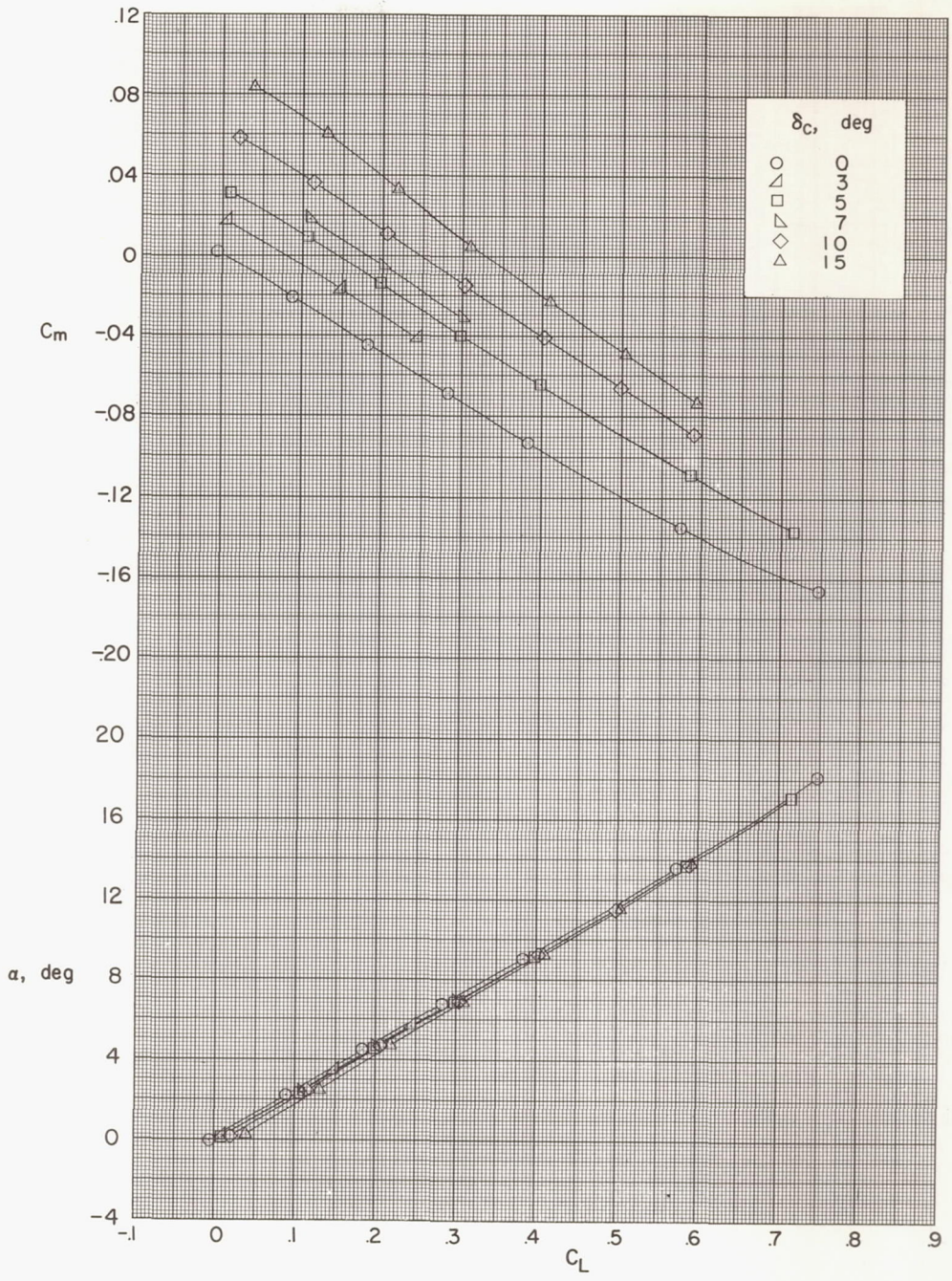

(a) Variation of C_m and α with C_L.

Figure 6.- Effect of canard-surface deflection on aerodynamic characteristics in pitch. High wing.

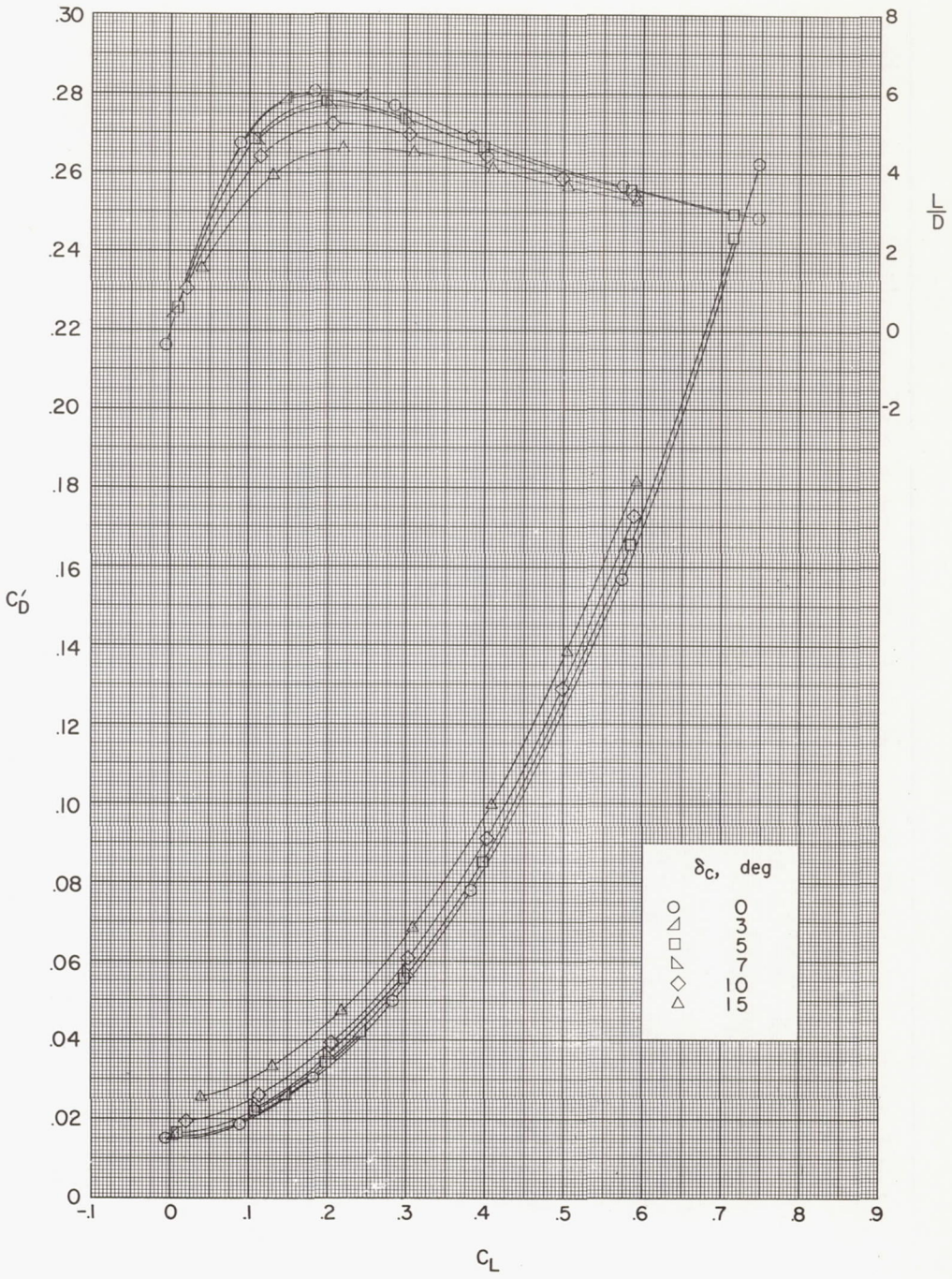

(b) Variation of L/D and C_D' with C_L.

Figure 6.- Concluded.

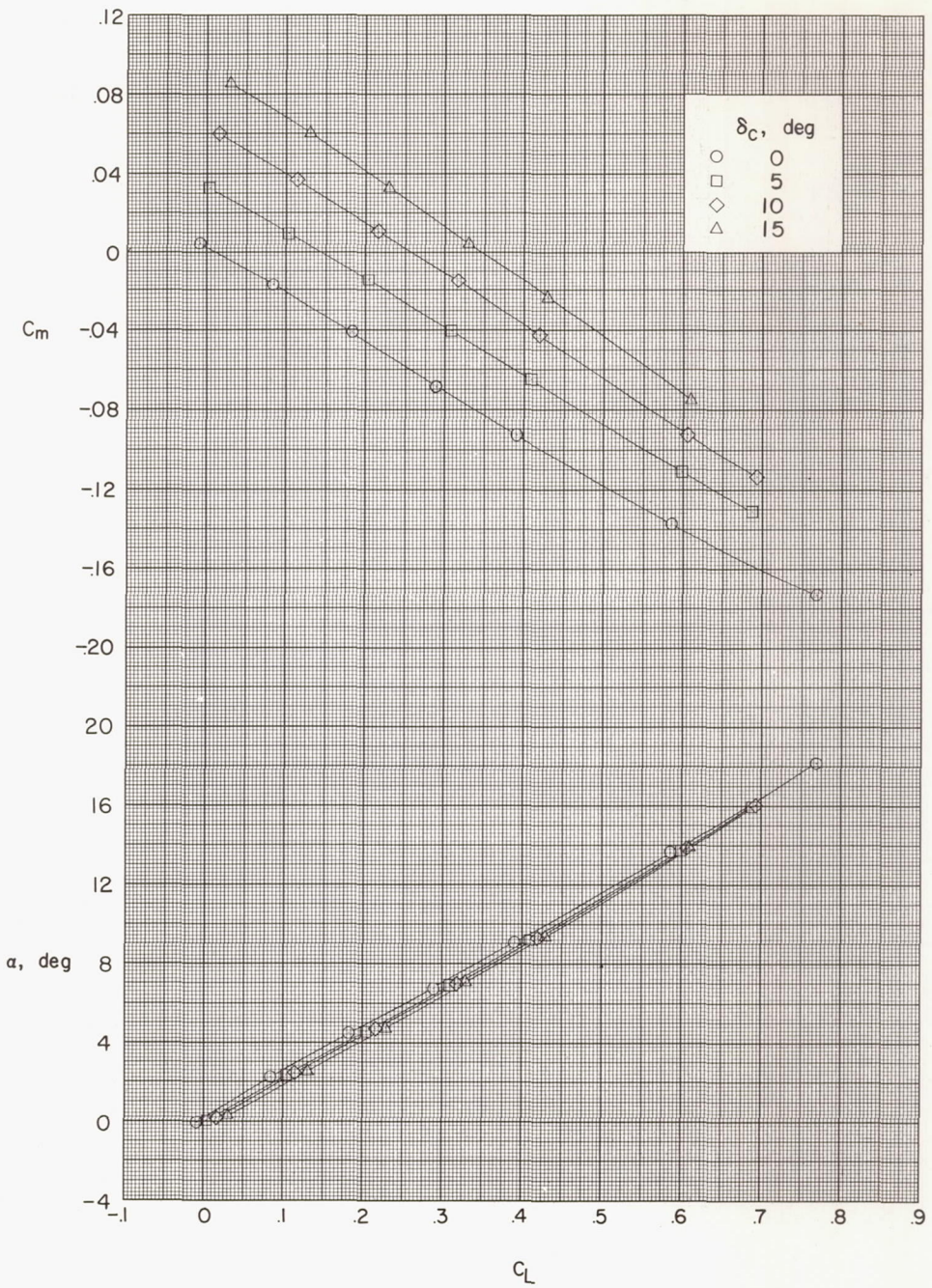

(a) Variation of C_m and α with C_L.

Figure 7.- Effect of canard-surface deflection on aerodynamic characteristics in pitch. Low wing.

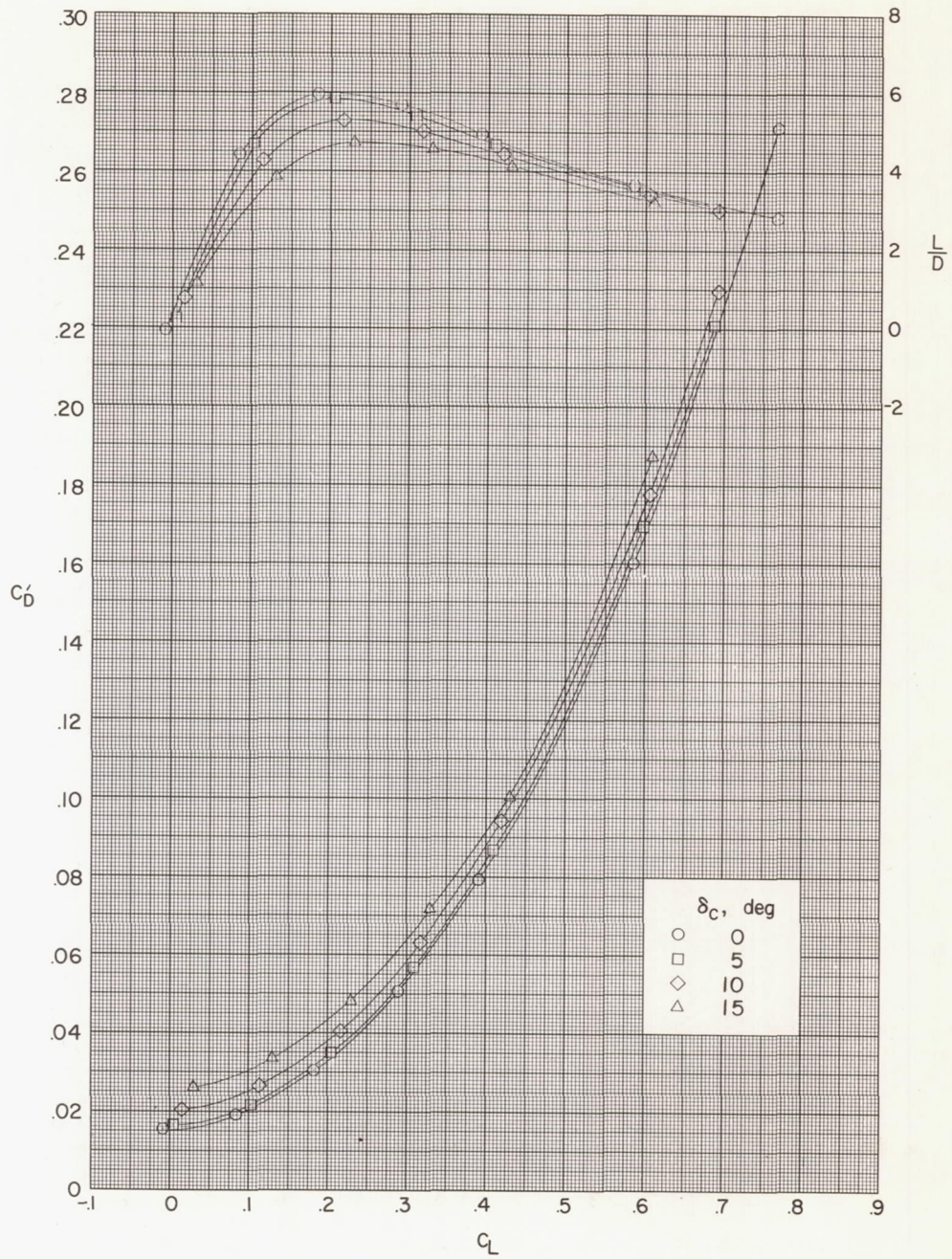

(b) Variation of L/D and C_D' with C_L.

Figure 7.- Concluded.

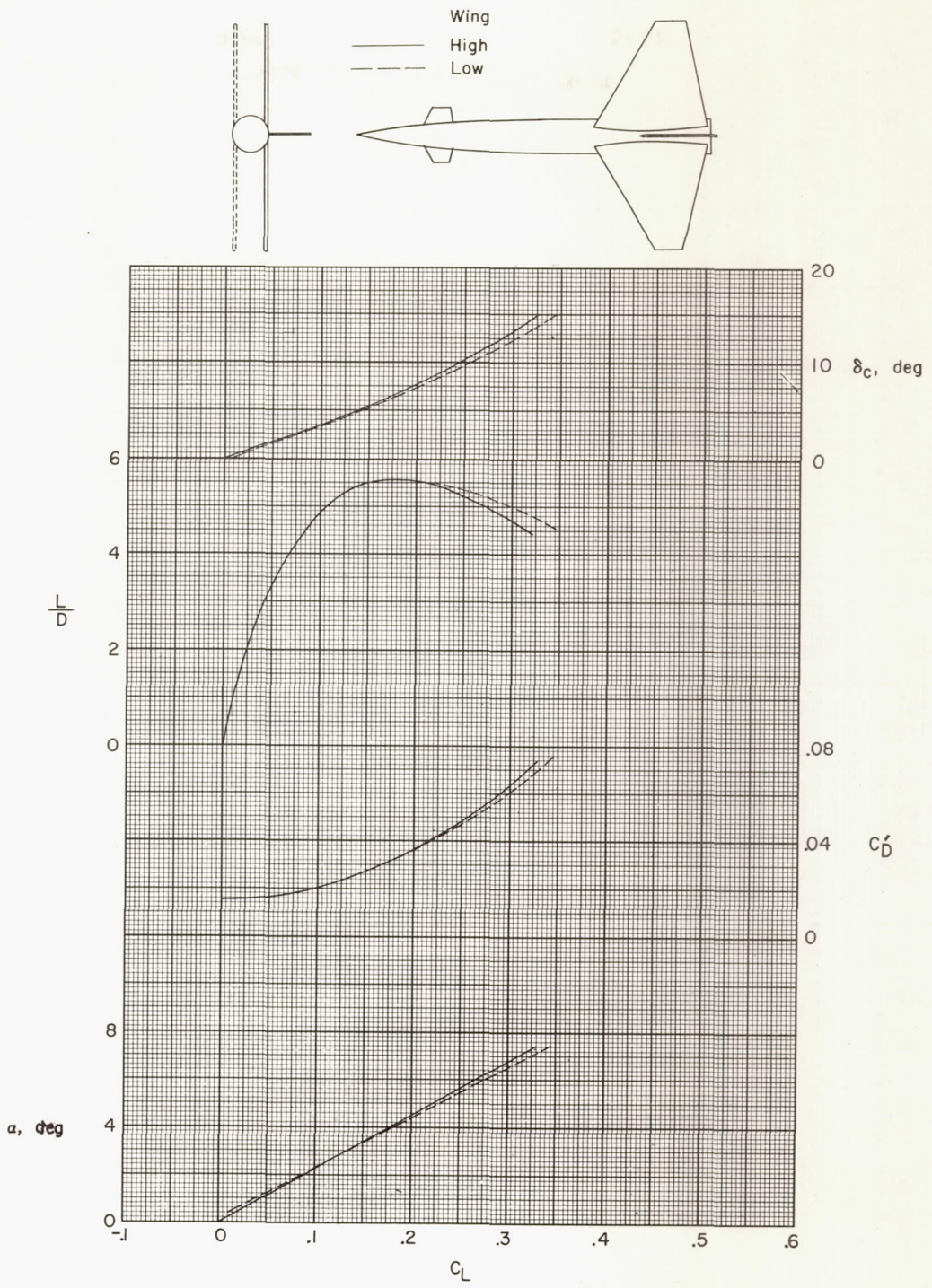

Figure 8.- Effect of wing vertical location on trim longitudinal characteristics. $\partial C_m/\partial C_L = -0.25$.

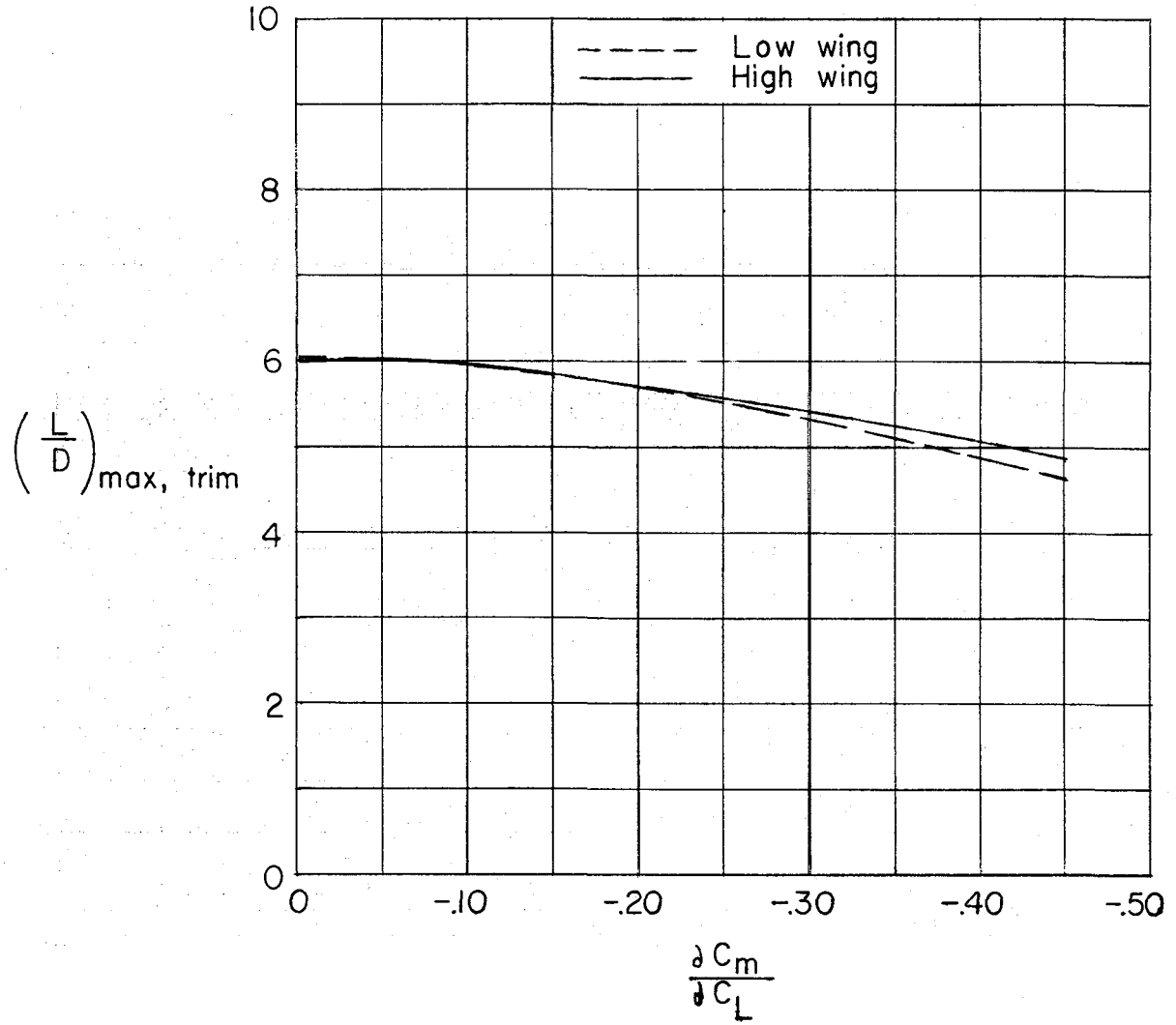

Figure 9.- Effect of wing vertical location on variation of maximum trimmed lift-drag ratio with longitudinal stability. WBCV.

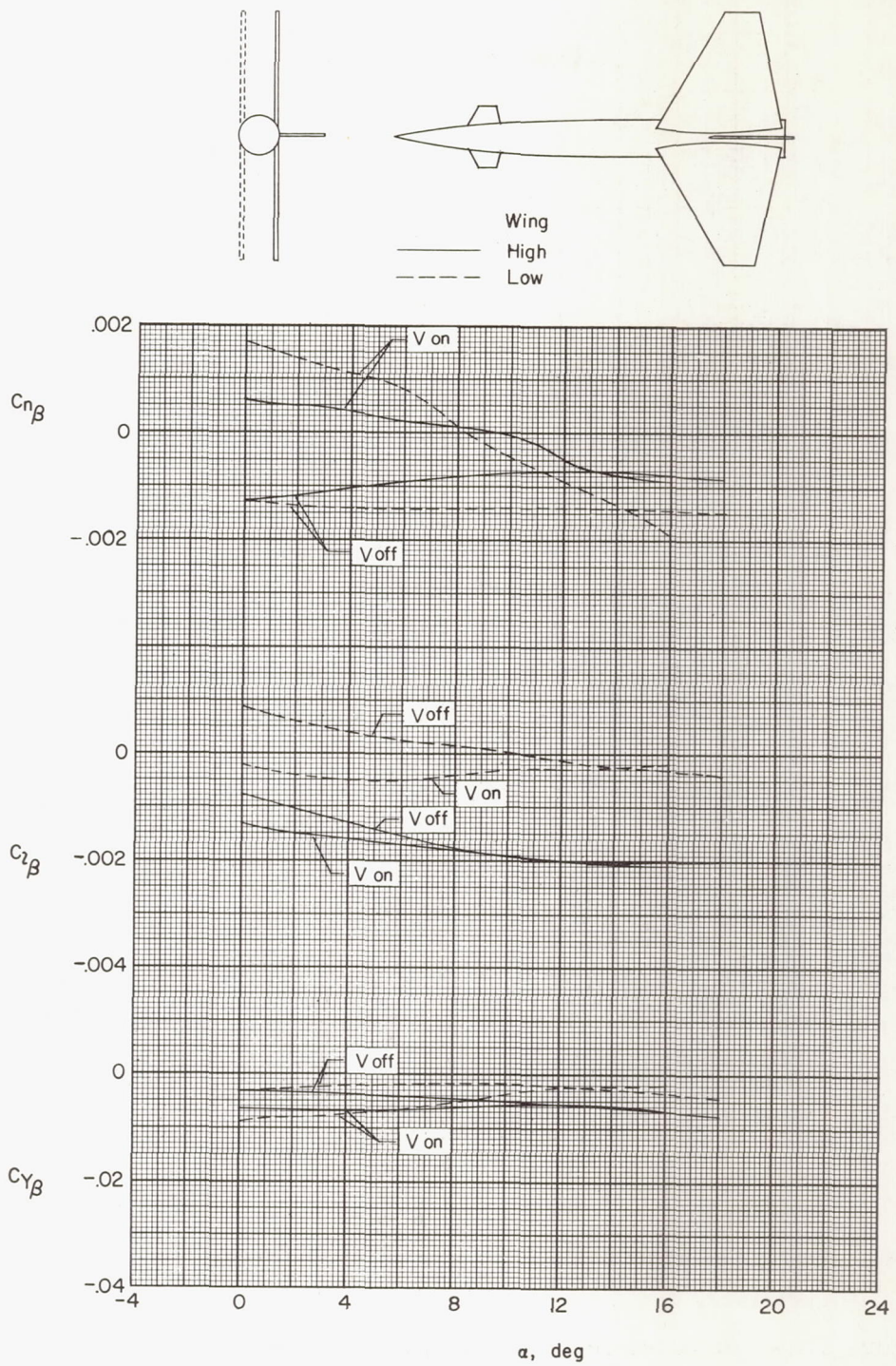

Figure 10.- Comparison of sideslip derivatives of high-wing and low-wing configurations with and without vertical tail. $\delta_c = 0^o$.

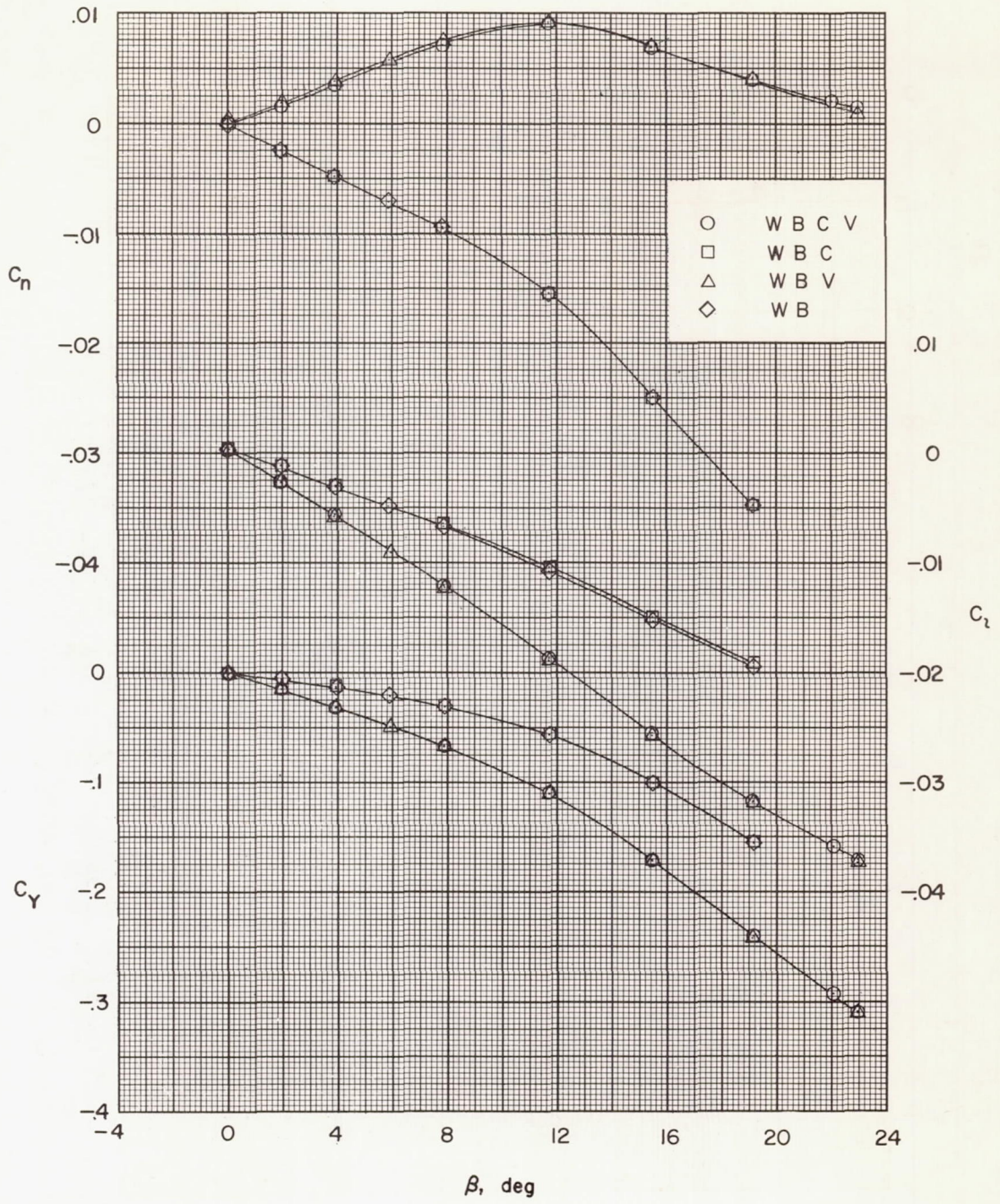

(a) $\alpha = 0^{\circ}$.

Figure 11.- Aerodynamic characteristics in sideslip for various combinations of components. High wing.

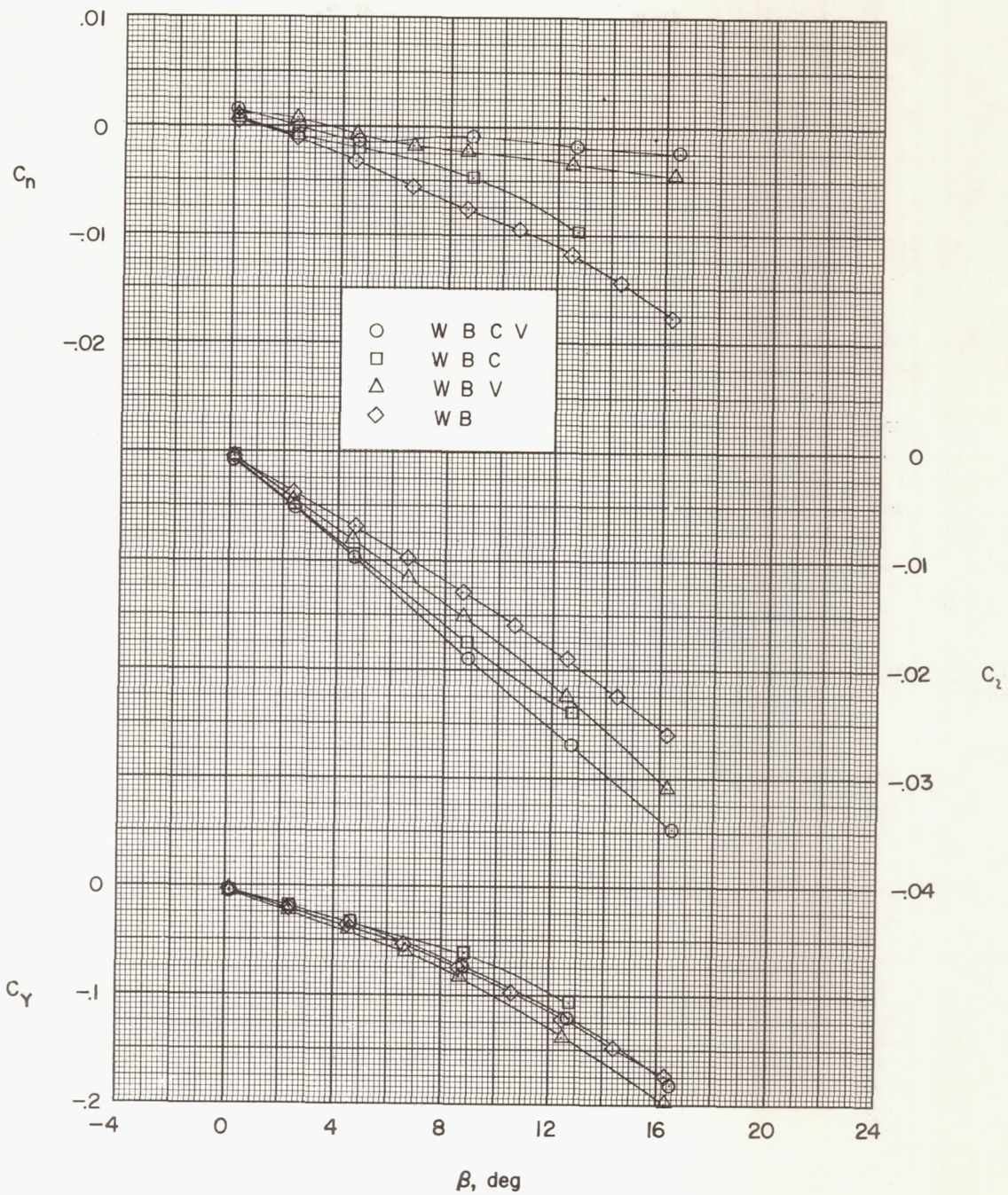

(b) $\alpha = 13.2^{\circ}$.

Figure 11.- Concluded.

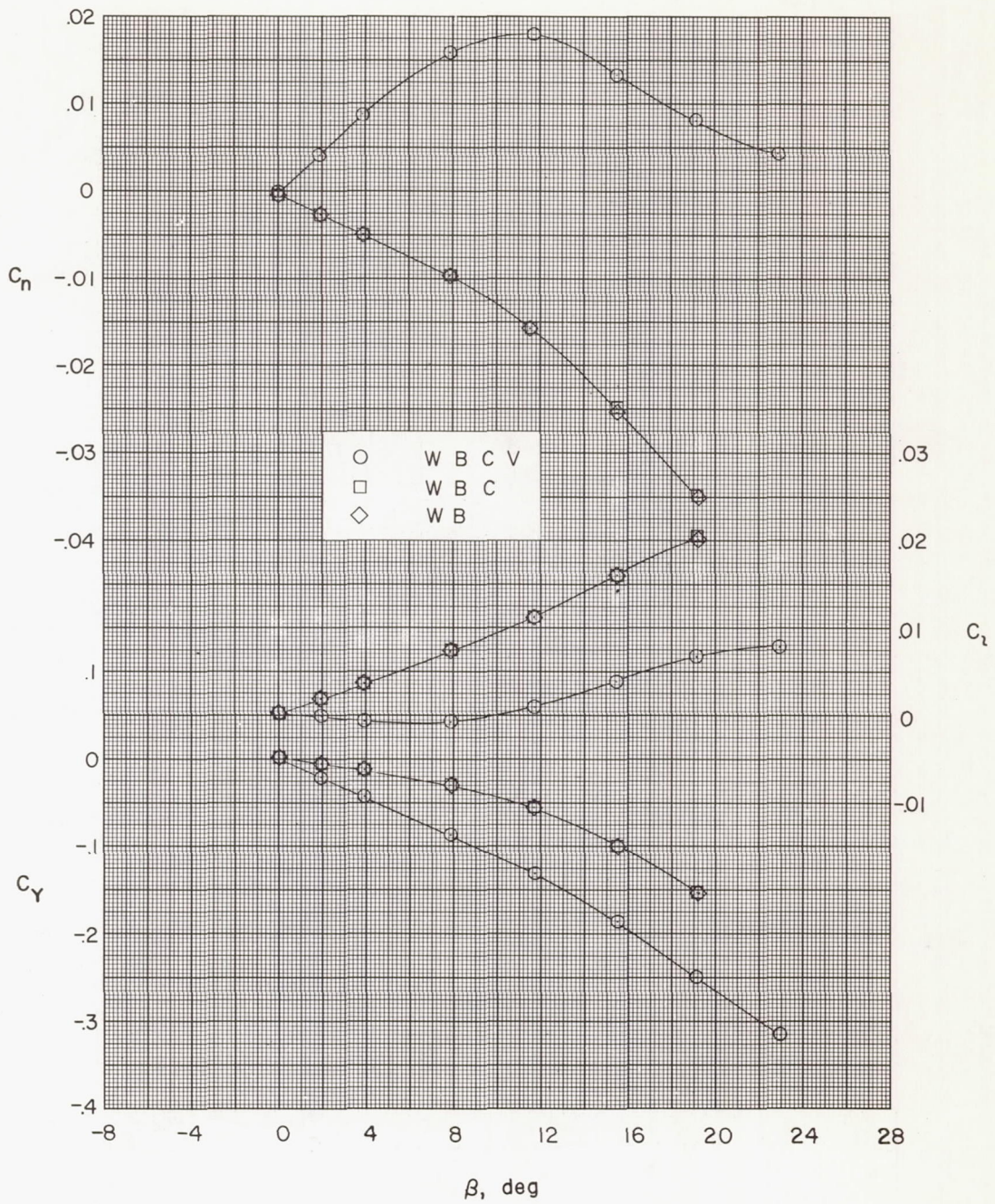

(a) $\alpha = 0^{\circ}$.

Figure 12.- Aerodynamic characteristics in sideslip for various combinations of components. Low wing.

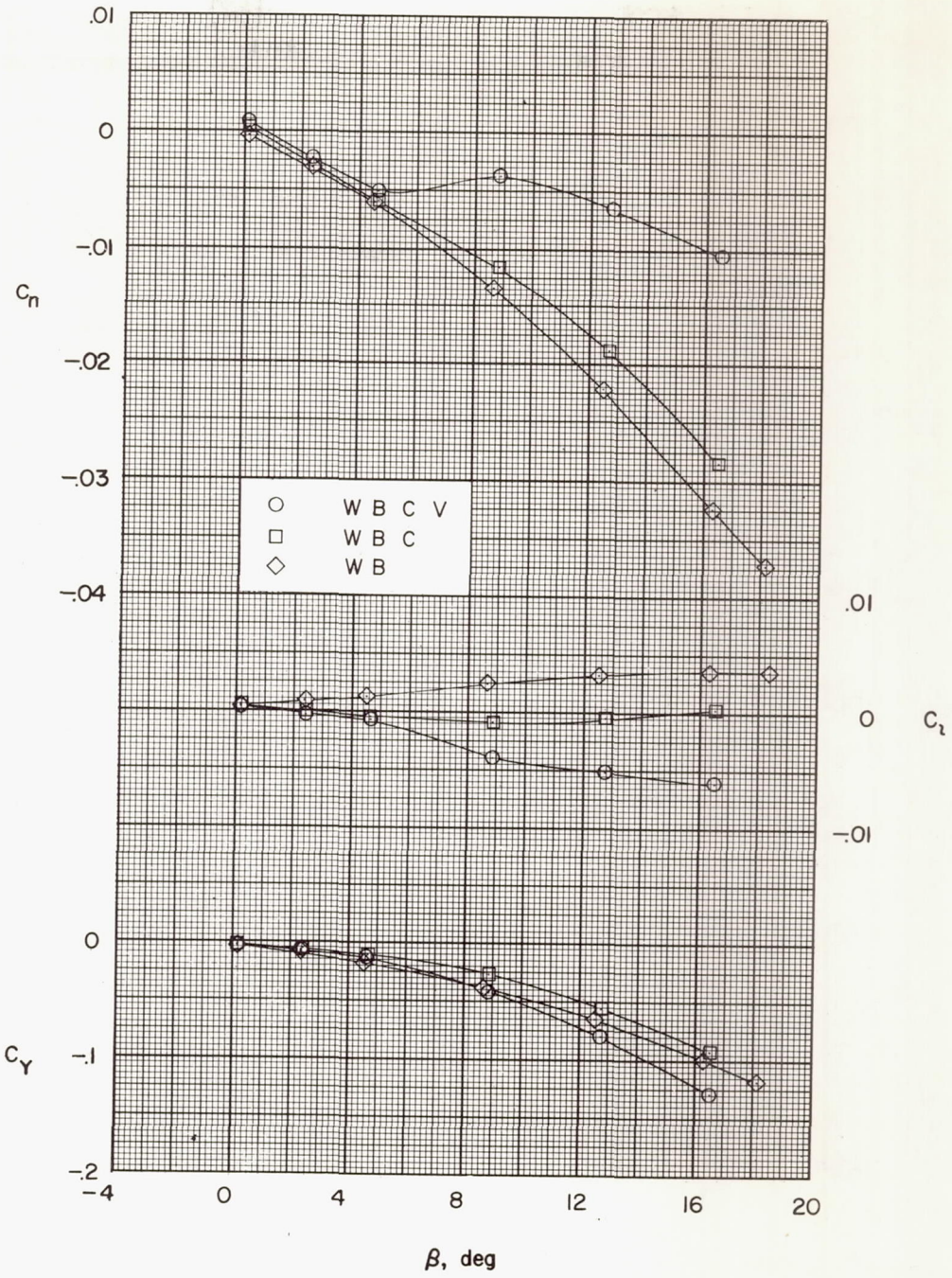

(b) $\alpha = 13.2^{\circ}$.

Figure 12.- Concluded.

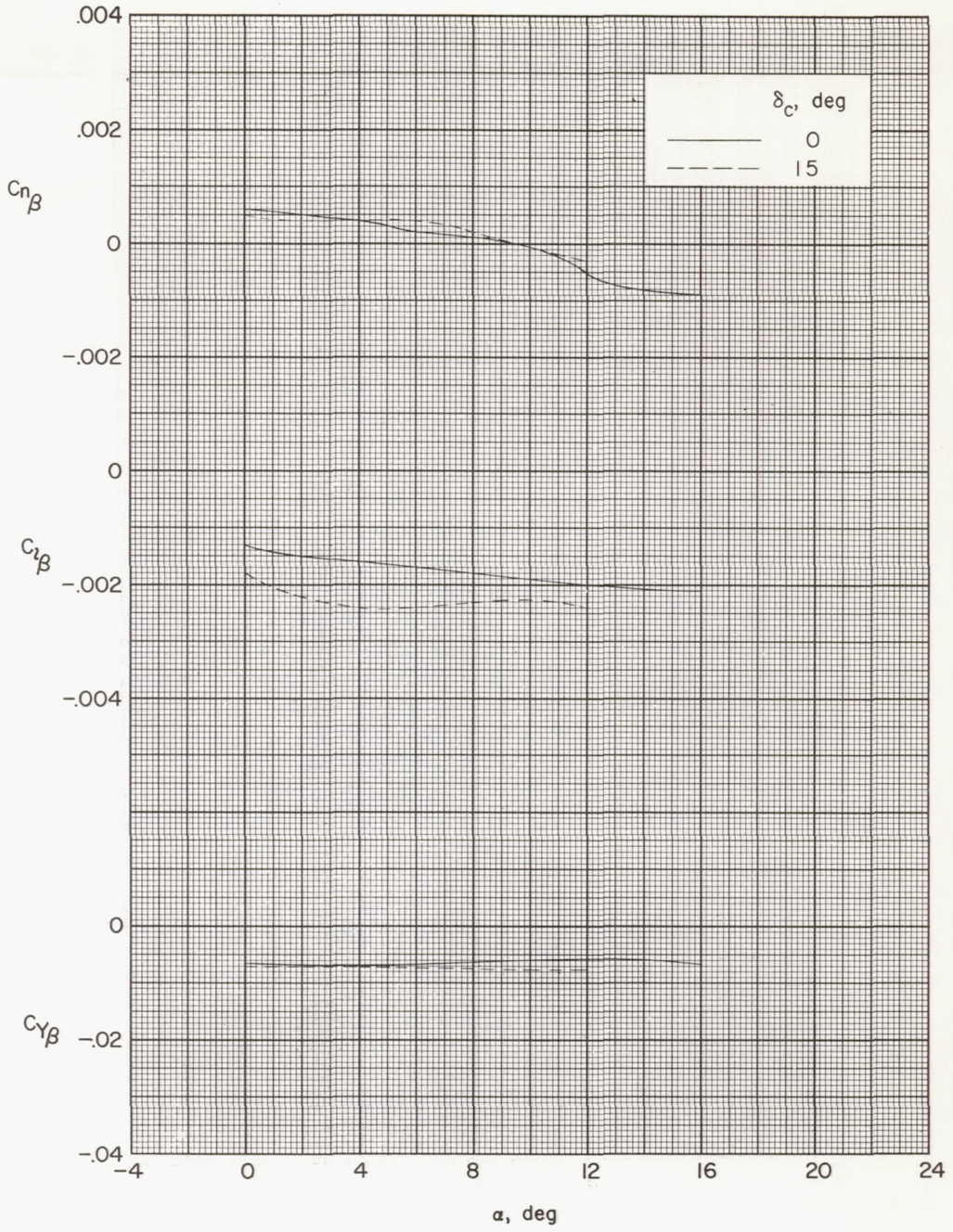

(a) High wing.

Figure 13.- Effect of canard-surface deflection on sideslip derivatives for complete model.

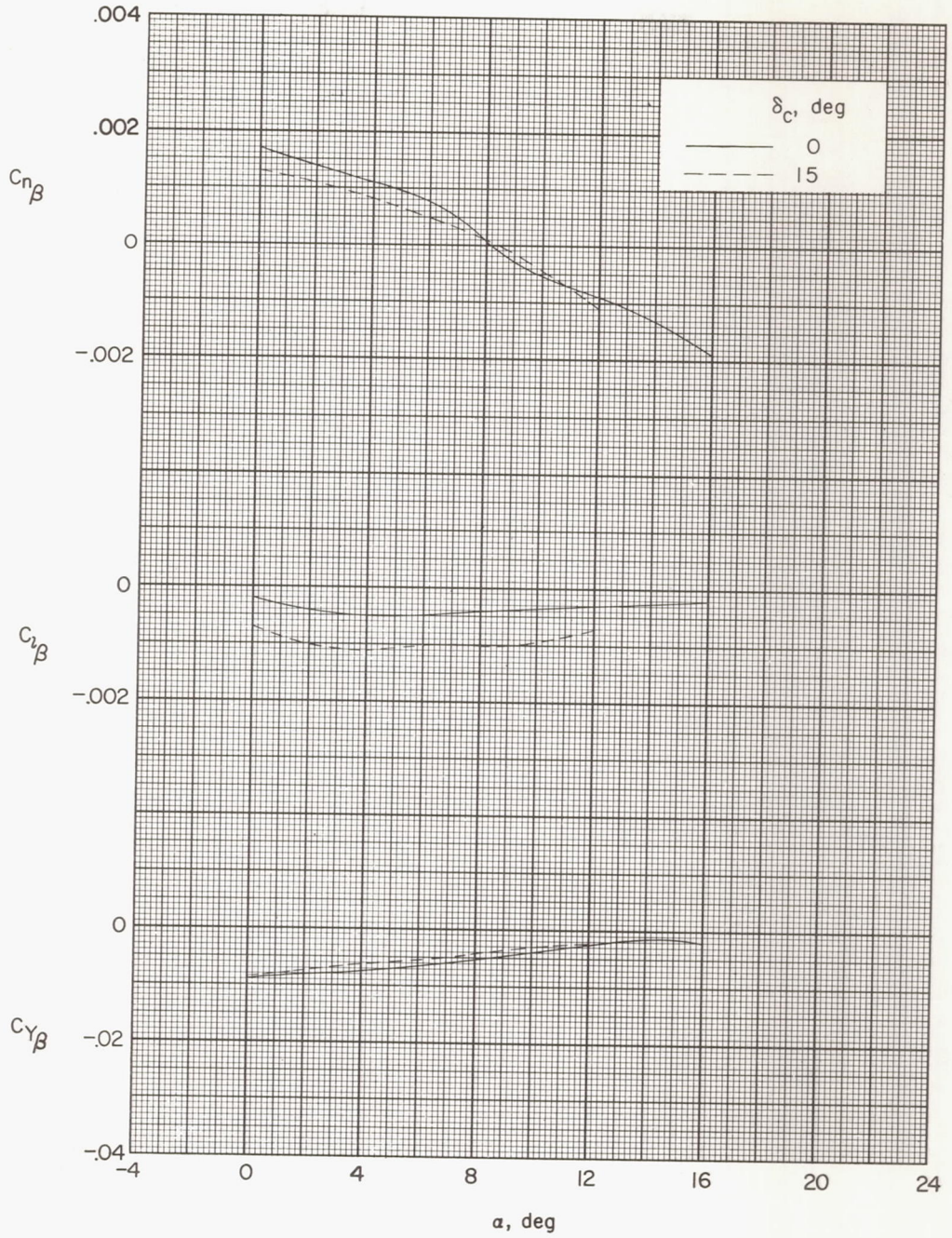

(b) Low wing.

Figure 13.- Concluded.